Localized Excitations in Arrays of Synchronized Laser Oscillators

Fabien Rogister[1,*] and Rajarshi Roy[2,†]

[1]TCTS Lab., Faculté Polytechnique de Mons, 31 boulevard Dolez, 7000 Mons, Belgium

[2]Institute for Physical Science and Technology and Department of Physics, University of Maryland, College Park, Maryland 20742, USA

(Received 17 November 2006; published 5 March 2007)

We investigate the spatiotemporal dynamics of a large array of laser oscillators. The oscillators are locally coupled and their natural frequencies are randomly detuned. We show that synchronization of the array elements results in localized excitations wandering along well-defined trajectories.

DOI: 10.1103/PhysRevLett.98.104101 PACS numbers: 05.45.Xt, 05.45.−a

The study of coupled nonlinear oscillators [1] provides insight to many complex phenomena observed in diverse natural and technological systems ranging from coupled neurons [2], arrays of Josephson junctions [3], and lasers [4,5]. The universal aspect of the synchronization of such arrays of oscillators can be explored in the combined perspectives of networks and nonlinear dynamics [6–10]. Investigations often aim at finding the conditions under which homogeneous states made of synchronized oscillators do appear and how spatial disorder in arrays of chaotic oscillators does induce regular patterns [11,12].

In this Letter, we examine two-dimensional arrays of locally-coupled laser oscillators with a random distribution of their natural optical frequencies. We show that collective dynamics results in the emergence of localized excitations. Unexpected in the presence of spatial randomness with large distribution widths, these coherent structures made of firing lasers wander along well-defined paths and can even rotate around periodic trajectories.

The formation of long-lived localized excitations is experimentally observed in very different physical systems—electrostatic oscillons on plasma-vacuum interfaces [13], oscillons in granular media [14], excitations in gas discharges [15,16], solitons on the surface of magnetic fluids [17], cavity solitons in nonlinear optics [18–21], as well as localized vegetation patches in ecosystems [22,23]. The nature of the interaction between neighboring spatial elements and the mechanisms for creation of localized excitations are obviously very different in each case. The discrete system considered in the following consists of a square array of $N = 2500$ (50×50) nonlinear laser oscillators. It can be realized with existing technology as shown in [24], although with a much smaller prototype. It is of interest for practical applications such as high-optical power emission. Indeed, the divergence of the overall beam emitted by an array of phase-locked lasers is strongly reduced, and the peak intensity resulting from the coherent superposition of the laser beams can scale as N^2 times the individual laser output (see Ref. [25] for an overview on this topic and Ref. [26] for the system considered here). The lasers are randomly detuned as would be the case in any experimental realization. The coupling is local and homogeneous: each elementary oscillator is coupled to its direct neighbors only and with an intensity that is not related to its position within the array. These features do not only simplify the numerical computation and the analysis of the results. They correspond also to experimental reality to a good approximation [24]. The system possesses dynamical variables with widely different time scales as well as controllable mechanisms for excitation and dissipation. Moreover, the coupling rate between neighboring elements may be varied over several orders. The equations for the slowly varying complex amplitudes $E_{i,j}$ of the electric fields inside the lasers and the equations for the corresponding population inversions $G_{i,j}$ are

$$\frac{dE_{i,j}}{dt} = (G_{i,j} - 1)E_{i,j} - \eta(E_{i-1,j} + E_{i+1,j} + E_{i,j-1} + E_{i,j+1}) + i\omega_{i,j}E_{i,j} \tag{1}$$

$$\frac{dG_{i,j}}{dt} = \gamma(p - G_{i,j} - G_{i,j}|E_{i,j}|^2), \tag{2}$$

where $1 < i, j < M$ with $M = 50$.

The dimensionless time t and the population inversion decay time γ^{-1} are measured in units of the field decay time. p is the pump coefficient. η is the normalized coupling rate between neighboring lasers. The normalized angular frequency $\omega_{i,j}$ measures the detuning of laser i, j from a common reference. Since the array extension is finite, lasers located on the boundary of the array are coupled to two or three neighbors, and the average intensity of their output is lower than the others. We point out that localized excitations can also be observed with periodic boundary conditions. In both cases, the array must be large enough to allow their generation. We assume a Gaussian detuning frequency distribution in the laser array, the other parameters being identical. The intensity of the light emitted by each laser (proportional to $|E_{i,j}|^2$) is stationary in the absence of detuning while detuned, the lasers can be driven unstable depending on the coupling rate [27]: if the interaction between lasers is weak, the individual optical phases are completely unlocked, and the laser intensities barely oscillate; however, if coupling is stronger than the so-called phase-locking threshold (see additional information in the auxiliary material to this Letter [28]; see

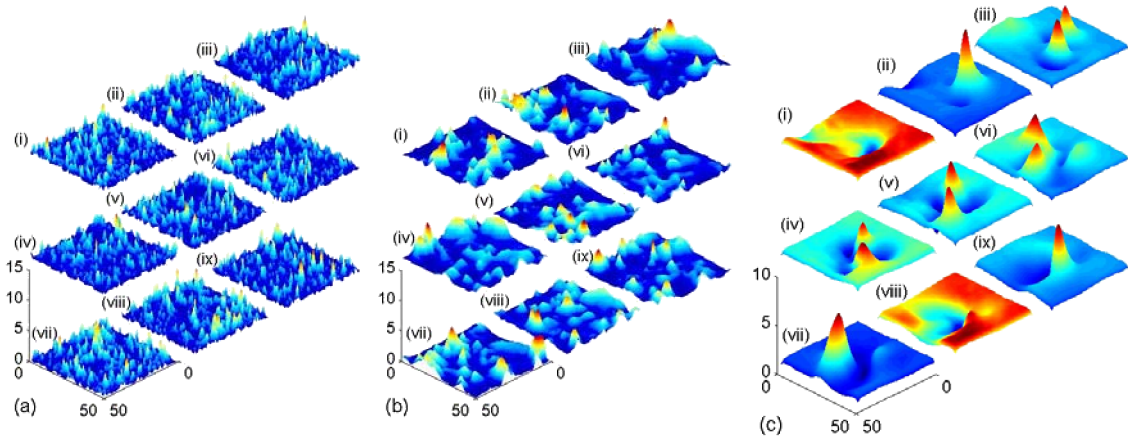

FIG. 1 (color online). Snapshots of intensity patterns at nine consecutive time steps over two relaxation oscillation periods of an uncoupled laser for three different values of the coupling rate, namely $\eta = 3.6 \times 10^{-3}$ (a), 1.6×10^{-2} (b), and 7×10^{-2} (c). The snapshots corresponding to $\eta = 7 \times 10^{-2}$ show the appearance of a localized excitation (ii) that splits into two new excitations (iii). Those travel across the array (iv–vi) and finally collide (vii) and fade (viii).

also Auxiliary Fig. 1), the lasers can operate in a state where the output intensities are constant and the optical phases perfectly locked. We have integrated Eqs. (1) and (2) by using a fourth order Runge-Kutta algorithm. We have used parameter values that are typical of solid-state lasers, namely $p = 2$ and $\gamma^{-1} = 1.2 \times 10^4$. For these values, the angular frequency of the relaxation oscillation [29] of an uncoupled laser is $\omega_R = 2\pi \times 2.06 \times 10^{-3}$, with $\omega_R = [2\gamma(p-1)]^{1/2}$. The detunings $\omega_{i,j}$ are chosen from a normal random distribution with mean zero. The distribution is generated by the *randn* MATLAB function for a given state of the generator. In most of the present Letter, the state of the generator is set to 1, the distribution standard deviation is $\sigma_\omega = 2\pi \times 5 \times 10^{-3}$, and the coupling rate ranges from moderate (i.e. strong enough to induce pulse dynamics) to values comparable to the phase-locking threshold. In most of this range, the array elements exhibit chaotic dynamics. Despite its simplicity, the model has been found to reproduce power-law spatial synchronization experimentally observed with small arrays [24].

For moderate coupling, the laser intensities display weakly synchronized chaotic trains of pulses with amplitudes and frequencies very different between neighboring elements. The patterns of the laser intensities are thus characterized by a large number of local maxima and the absence of continuity [Fig. 1(a) and movie no. 1 in Ref. [28]]. For increasing coupling rates, the laser intensity oscillations slow down, and their mean frequencies get closer. In addition, the offset between phase and amplitude of neighbors decreases. As a result of synchronization over an increasing spatial range, the number of local maxima decreases rapidly [Fig. 2(a)], and the patterns gradually acquire spatial continuity. Figure 1(b) and movie no. 2 in Ref. [28] provide an example of the dynamics for an intermediate value of η. The laser behavior depends more and more on their location in the lattice as the coupling rate gets closer and closer to the phase-locking threshold. On the array scale, the collective dynamics results in the emergence of a few spatially localized excitations made of momentarily firing lasers [Fig. 1(c) and movie no. 3 in Ref. [28]]. These excitations remain during long periods and move over large distances across a weakly oscillating background. They can directly emerge from this background or result from the splitting of previous excitations. Two excitations can also collide.

The pattern spatial coherence is estimated by computing the time-averaged full width at half maximum of the two-dimensional autocorrelation function. This function characterizes the extent to which oscillators separated by a given distance oscillate in unison at a given time (the Auxiliary Figures 2 (a–c) in Ref. [28] present this function calculated for three different patterns). Figure 2(b) displays the mean correlation length of the patterns with respect to the coupling rate. Comparison with Fig. 2(a) shows how the increase of the correlation length is associated with the reduction of the number of local maxima and therefore with the gradual organization of the firing lasers in a few spatially localized excitations. For the lowest value of the coupling rate considered, the correlation length is smaller than 2 array sites, and the mean number of maxima is over 60, revealing the almost free motion of the oscillators. As the coupling increases, the correlation length and the number of maxima, respectively, increase and decrease rapidly: the spatial continuity of the patterns improves and finally saturates. Just below the phase-locking threshold, the number of excitations is less than 1.5 on average, and the correlation length of the patterns is over 10 array sites, indicating a long-range spatial synchronization.

The progressive synchronization of the lasers also affects the velocity of the excitations across the array: the mean velocity of the pattern maxima increases with the

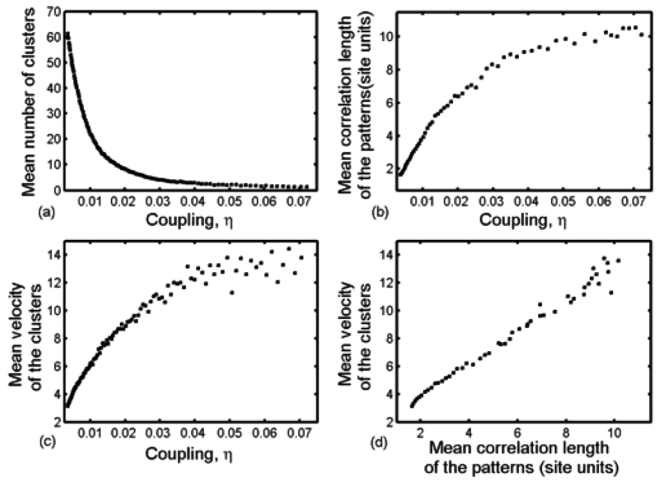

FIG. 2. Mean number of clusters made of firing lasers (a), mean correlation length of the intensity patterns (b), and mean velocity of the clusters across the laser array (c) as functions of the coupling rate, η. Mean velocity of the clusters versus the mean correlation length of the intensity patterns (d). The mean numbers of clusters and their mean velocities are calculated from the same five time series, each of duration equivalent to 30 relaxation oscillation periods of an uncoupled laser. The mean correlation lengths of the patterns are calculated from five time series of duration equivalent to ten relaxation oscillation periods.

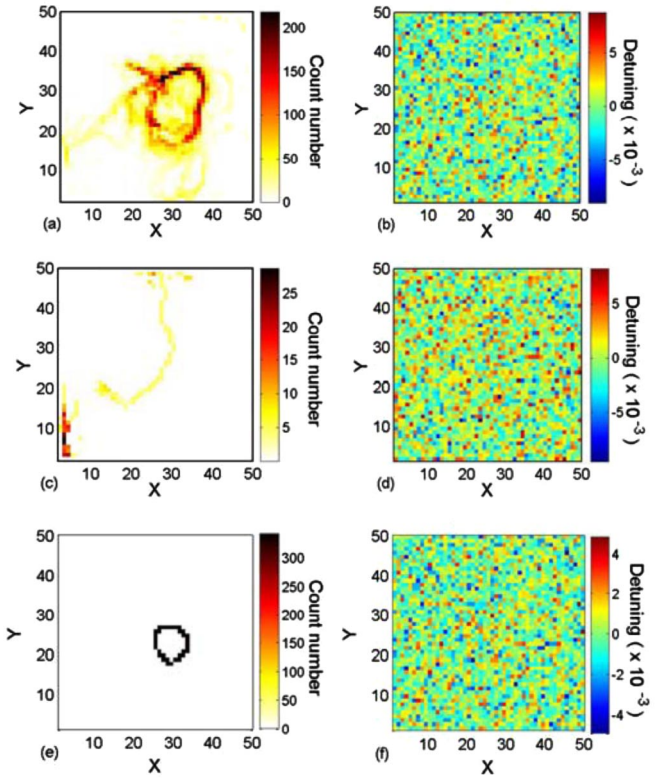

FIG. 3 (color online). (a) Histogram showing the number of times each site of the array is visited by the peak of a localized excitation for $\eta = 7 \times 10^{-2}$. (b) Realization of a normal random distribution with mean zero and standard deviation of $\sigma_\omega = 2\pi \times 5 \times 10^{-3}$. The realization is generated by the *randn* MATLAB function. The state of the random generator was set to 1. (c) and (d): same as in (a) and (b), but the state of the random generator was set to 2. (e) and (f): same as in (a) and (b), but with $\sigma_\omega = 2\pi \times 2.76 \times 10^{-3}$ and $\eta = 6.2 \times 10^{-2}$. The histograms have been averaged over 5 time series. The duration of each series corresponds to 500 periods of the relaxation oscillations of an uncoupled laser.

coupling rate and progressively saturates [Fig. 2(c)] similarly to the correlation length. Figure 2(d) reveals an almost linear relationship between the correlation length and the excitation mean velocity; thus, both features benefit similarly from the long-range spatiotemporal synchronization between the lasers.

Close to the phase-locking threshold, the dynamics of the array elements is still aperiodic and the trajectories of the excitations in the array cannot be anticipated on a long-term basis. It is however apparent from their observation over long periods that they have a strong propensity to follow a few well-defined paths (see movie no. 3 in Ref. [28]). In order to substantiate this qualitative observation, we have computed a histogram of the trajectories of each localized excitation by recording the number of times they visit the different cells of the array over 500 relaxation oscillation periods of an uncoupled laser. The histogram displayed in Fig. 3(a) shows that a large part of the lattice is never visited. The most visited cells form a ring. The localized excitations are typically generated in the darker zones of the histogram located on the top of the ring and generally follow either the left part of the ring anticlockwise or the right part clockwise. From time to time, the excitations also follow two other paths that lead toward the array boundaries close to which they decrease in amplitude and finally blend in with the background fluctuations. On occasion, the excitations can escape from the most likely paths but, after what looks like a short hesitancy, move back toward these corridors.

Although there is no obvious relationship between the layout of the trajectories and the distribution of the detuning shown in Fig. 3(b), different realizations of the distribution lead to completely different layouts. As a first example, Figs. 3(c) and 3(d) compare the trajectory layout and the detuning distribution when the state of the random generator is set to 2. In this case, the laser dynamics is periodic. The lasers located in a corner of the array exhibit large fluctuations, and a single localized excitation forms close to this region, moves toward the central part of the array, and then turns left and finally evaporates on an edge (see movie no. 4 in Ref. [28]). In Figs. 3(e) and 3(f), the state of the generator is again set to 1, but the standard deviation and the coupling are reduced. One now observes a unique excitation periodically rotating around a closed trajectory (see movie no. 5 in Ref. [28]). Again, there is apparently no relationship between this trajectory and the spatial distribution of the detuning. Multiple numerical

simulations reveal that in every case, the trajectory layout is robust to slight (of the order of a few percents) random modifications of the laser detuning and to a few array defects. The most visited paths are best defined for large coupling. For decreasing coupling rate, the histograms fade, the number of paths increases, and the excitation trajectories cover the array in a more and more homogeneous manner; at the same time, the firing lasers are less localized as the whole array fluctuates strongly.

In summary, localized excitations wandering along well-defined trajectories can emerge in spatially disordered arrays of laser oscillators. They are an unexpected consequence of spatial synchronization that progressively takes place when the interaction between the array elements increases. The simplicity of the model suggests that synchronization-induced localized excitations should take place in a wide variety of natural and laboratory systems where spatial randomness is also unavoidable. The comparison with pacemaker models that assume locally-coupled firing cells with random detuning of their natural oscillation frequencies deserves discussion. Indeed, to the best of our knowledge, the firing of cells appears as spreading waves [30] instead of localized excitations. We think that this is due to the intrinsic features of the cells that, contrary to the laser oscillators, already fire periodically in the absence of coupling. When coupled, spreading waves are generated as the excitation of a cell triggers the excitation of the following ones [30]. In the system here under study, firing requires interaction between lasers.

F. R. and R. R. respectively acknowledge support from the Fonds National de la Recherche Scientifique and the Physics Division of the Office for Naval Research.

*Electronic mail: rogister.f@belgacom.net
†Electronic mail: rroy@glue.umd.edu

[1] Y. Kuramoto, *Chemical Oscillations, Waves and Turbulence* (Springer, Berlin, 1984).
[2] E. Barreto, P. So, B. J. Gluckman, and S. J. Schiff, Phys. Rev. Lett. **84**, 1689 (2000); B. J. Gluckman, T. I. Netoff, E. J. Neel, W. L. Ditto, M. L. Spano, and S. J. Schiff, Phys. Rev. Lett. **77**, 4098 (1996).
[3] K. Wiesenfeld, P. Colet, and S. H. Strogatz, Phys. Rev. E **57**, 1563 (1998).
[4] H. G. Winful and S. S. Wang, Appl. Phys. Lett. **53**, 1894 (1988).
[5] L. Fabiny, P. Colet, R. Roy, and D. Lenstra, Phys. Rev. A **47**, 4287 (1993).
[6] S. H. Strogatz, Nature (London) **410**, 268 (2001).
[7] S. Boccaletti, V. Latora, Y. Moreno, M. Chavez, and D.-U. Hwang, Phys. Rep. **424**, 175 (2006).
[8] D. J. Watts and S. H. Strogatz, Nature (London) **393**, 440 (1998).
[9] J. G. Restrepo, E. Ott, and B. R. Hunt, Phys. Rev. E **71**, 036151 (2005).
[10] M. Barahona and L. M. Pecora, Phys. Rev. Lett. **89**, 054101 (2002).
[11] Y. Braiman, J. F. Lindner, and W. L. Ditto, Nature (London) **378**, 465 (1995).
[12] This observation inspired many other studies. The role of spatial disorder in arrays of oscillators has been studied for example in the following papers: G. V. Osipov, A. S. Pikovsky, M. G. Rosenblum, and J. Kurths, Phys. Rev. E **55**, 2353 (1997); N. V. Alexeeva, I. V. Barashenkov, and G. P. Tsironis, Phys. Rev. Lett. **84**, 3053 (2000); A. Gavrielides, T. Kottos, V. Kovanis, and G. P. Tsironis, Phys. Rev. E **58**, 5529 (1998); M. Weiss, T. Kottos, and T. Geisel, Phys. Rev. E **63**, 056211 (2001).
[13] L. Stenflo and M. Y. Yu, Phys. Fluids B **1**, 1543 (1989); B. B. Chakraborty, Phys. Fluids B **3**, 857 (1991); L. Stenflo and M. Y. Yu, Nature (London) **384**, 224 (1996); L. Stenflo and M. Y. Yu, Phys. Plasmas **5**, 3122 (1998).
[14] P. B. Umbanhowar, F. Melo, and H. L. Swinney, Nature (London) **382**, 793 (1996).
[15] Y. A. Astrov and Y. A. Logvin, Phys. Rev. Lett. **79**, 2983 (1997).
[16] I. Müller, E. Ammelt, and H.-G. Purwins, Phys. Rev. Lett. **82**, 3428 (1999).
[17] R. Richter and I. V. Barashenkov, Phys. Rev. Lett. **94**, 184503 (2005).
[18] D. W. Mc Laughlin, J. V. Moloney, and A. C. Newell, Phys. Rev. Lett. **51**, 75 (1983).
[19] N. N. Rosanov and G. V. Khodova, Opt. Spectrosc. **65**, 449 (1988).
[20] M. Saffman, D. Montgomery, and D. Z. Anderson, Opt. Lett. **19**, 518 (1994).
[21] S. Barland *et al.*, Nature (London) **419**, 699 (2002).
[22] O. Lejeune, M. Tlidi, and P. Couteron, Phys. Rev. E **66**, 010901(R) (2002).
[23] M. Rietkerk, S. C. Dekker, P. C. de Ruiter, and J. van de Koppel, Science **305**, 1926 (2004).
[24] F. Rogister, K. S. Thornburg, L. Fabiny, M. Möller, and R. Roy, Phys. Rev. Lett. **92**, 093905 (2004).
[25] *Diode Laser Arrays*, edited by D. Botez and D. R. Scifres (Cambridge Univ. Press, Cambridge, 1994).
[26] F. Rogister and R. Roy, Laser Phys. **15**, 313 (2005).
[27] K. S. Thornburg, M. Möller, R. Roy, T. W. Carr, R.-D. Li, and T. Erneux, Phys. Rev. E **55**, 3865 (1997).
[28] See EPAPS Document No. E-PRLTAO-98-069710 for the auxiliary material. It contains information on the phase-locking threshold, supplementary figures and movies showing the laser array dynamics. For more information on EPAPS, see http://www.aip.org/pubservs/epaps.html.
[29] The relaxation oscillations result from the exchange of energy between the population inversion and the electromagnetic field inside the laser cavity.
[30] J. Keener and J. Sneyd, *Mathematical Physiology* (Springer, Berlin, 1998).